IJISET - International Journal of Innovative Science, Engineering & Technology, Vol. 8 Issue 2, February 2021
ISSN (Online) 2348 – 7968 | Impact Factor (2020) – 6.72
www.ijiset.com

Optical, Structural and Morphological Analysis of rGO Decorated $CoSe_2$ Nanocomposites

K. Mahalakshmi[1], V. Lakshmi[1], S. Dhivya christo anitha[1] and Dr. R. MaryJenila[2]

[1] Research Scholar, Department of Physics, St.Xavier's College (autonomous), Palayamkottai, 627002, India
[2]Assistant Professor, Department of Physics, St.Xavier's College (autonomous), Palayamkottai, 627002, India

Abstract

The incorporation of two-dimensional (2-D) graphene and layered transition metal dichalcogenides has considered as one of the essential nanocomposites for obtaining energy storage devices. Graphite materials is extensively used in the Li-ion batteries because of its good durability and light weight. In order to improve the performance of the graphite materials, the transition metal dichalcogenides has been decorated over the surface of reduced graphene oxide. Among transition metal chalcogenide, cobalt selenide has been chosen for this work. In this study, rGO decorated $CoSe_2$ nanocomposites were synthesized via facile hydrothermal method. The properties of these nanocomposites have been studied using different characterization techniques such as X-ray diffraction (XRD), Scanning Electron Microscopy (SEM-EDAX), Fourier Transform Infrared spectroscopy (FTIR), UV-VIS spectroscopy. From the XRD spectra, the average grain size is found to 18.63nm. The optical bandgap of the synthesized nanocomposites is determined from UV –visible absorption spectrum.

Keywords: ***reduced graphene oxide; cobalt Selenide; hydrothermal method; energy storage.***

1. Introduction

Carbon is the most essential part of all allotropic carbonic constituents. Among them, graphene and its derivatives graphene oxide (GO) and Reduced Graphene Oxide(rGO) was familiar [1]. Graphene is a two-dimensional (2D) material made up of sp2 hybridized carbon atoms which disposed in a hexagonal packing that was theoretically predicted long time ago [2]. Graphene is considered the thinnest stretchable material having good thermal conductivity and high electron mobility [3]. Graphene and its derivatives such as graphene oxide (GO) and reduced graphene oxide (rGO) has involved great interest in both fundamental science and technology due to their exciting structures and excellent electronical, mechanical and thermal properties. GO involves many functionalized groups, where most of them contain carboxylic and hydroxylic groups. This reveals their surface fictionalization role for numerous applications. [4,5]. In addition, GO and its composites have been shown to be essential for tumor targeting effect and higher tumor uptake due to its improved permeability [6,7]. Reduced graphene oxide has comparable mechanical, optoelectronic and conductive properties like graphene because it possesses a heterogeneous structure comprised of a graphene-like basal plane. In addition, it is decorated with structural defects and inhabited with areas containing oxidized chemical groups. The graphene-like properties made reduced graphene oxide a highly required material to be used in the optoelectronic and storage devices [8]. Reduced graphene oxide (rGO) is a unique structure which illustrates strong interaction between the carbon–carbon interlayers and shows low energy photons in the infrared region [9]. On the other hand, CoSe2 has drawn much consideration in recent years, because of its admirable properties as an electrocatalyst for the hydrogen evolution reaction [10], oxygen evolution reaction [11] and application in dye sensitized solar cells [12]. The inorganic material cobalt selenide possesses an optimal band gap which is well matched

with the solar spectrum due to its high optical absorption coefficient and good conductivity. These features make it relatively suitable for use as a photo-electrode in solar conversion devices [13]. Cobalt selenide provides high current density at low coverage so it can be used in the energy storage devices. However, to the best of our knowledge, there is only a few works reported on the synthesis of rGO decorated CoSe2 nanocomposites [15]. Moreover, the study uncovered the detailed analysis of optical properties of the nanocomposites. In this work, we present a facile process to synthesis rGO decorated CoSe2 nanocomposites. A two-dimensional structure of graphene was attached to the Cobalt Selenide by hydrothermal process. The prepared composites were subjected to structural and optical studies. Furthermore, the prepared composites show good band gap of 1.4eV. There is a report that cobalt selenide has a band gap of 1.8ev [16]. By adding rGO to cobalt selenide it reduced the size of the nanocomposites, it made the composites to increase its specific capacitance.

2. Materials and methods

2.1. Materials

rGO decorated $CoSe_2$ nanocomposites were prepared via facile hydrothermal reaction using graphene oxide, Cobalt Acetate (Co $(CH_3COO)_2.4H_2O$), selenium powder and hydrazine hydrate as starting materials. In this work, there are two steps involved in the synthesis of rGO decorated $CoSe_2$ nanocomposites. The first step involved the synthesis of graphene oxide. The second step involved the synthesis of rGO decorated $CoSe_2$ nanocomposites from the prepared graphene oxide, Cobalt Acetate and Selenide using the reducing agent hydrazine hydrate.

2.2. Synthesis of Graphene Oxide

4g of Graphite and 2g of Sodium Nitrate ($NaNo_3$) were mixed with 100 ml Sulphuric acid followed by stirring at 400 rpm for 5 h in an ice bath. After that 15 g of potassium permanganate ($KMnO_4$) and 200 ml of distilled water were added very slowly while it was being stirred for 3 h at 20° C. The temperate was then increased to 30° C and continuously stirred for 3 h. Next the mixture was refluxed at 100° C for 30 min. Then change the temperature to 25° C for another 15 min. Again, change the temperature to 20° C and leave it for 3 h. Then the solution was added to 50 ml of hydrogen peroxide (H_2O_2) and it became yellowish in colour. After that 200ml of distilled water was poured into the prepared mixture and stirred for 2 h. Then the precipitate was collected and washed with 10% of hydrochloric acid and then it is washed with distilled water several times. The final product was dried at 60° C for 2 d to obtain GO.

2.3. Synthesis of rGO decorated $CoSe_2$ Nanocomposites

rGO decorated $CoSe_2$ nanocomposites were synthesized via facile hydrothermal process. GO powder (50 mg) was dispersed in 25ml distilled water using ultrasonicator for 8h. After ultrasonication, 1mmol of Cobalt Acetate (Co $(CH_3COO)_2.4H_2O$) and Selenium powder were added and stirred for 5 h followed by the addition 0f 1 ml of hydrazine hydrate ($N_2H_4.H_2O$). After more than 5 h stirring, the mixture precursor solution was transferred to 100 ml Teflon lined autoclave and heated at 200°C for 1 d. The resultant slurry was centrifuged and washed several times with distilled water and ethanol. Then the products were collected and dried in an oven at 300° C Overnight.

2.4. Characterization techniques

The synthesized nanocomposites are subjected to various analyses. X-ray diffraction (XRD) (Xpert pro, PAN analytical Philips) was used to investigate the structure of the synthesized samples. Powder samples were exposed to CuKα radiation at 1540Å. Samples were examined in the range from 0̊ to 90̊. The microstructure and morphology of the synthesized samples was examined with scanning electron microscopy (SEM). The functional groups present in the samples were studied by the emission or absorption of infrared spectra using Fourier –transform infrared spectroscopy (FTIR) (IRTracer-100-shimadzu). The optical properties of the synthesized samples were studied by UV-Vis spectrometer (UV-3600plus-Shimadzu) in the range of 200-1600 nm. The obtained results are discussed in detail below.

3. Results and Discussions.

3.1. Identification of the structure of rGO decorated $CoSe_2$ Nanocomposites

The XRD pattern of GO and rGO decorated $CoSe_2$ Nanocomposites are shown in the fig.1. In the XRD pattern of GO, the peak at 11.7º corresponds to an interlayer distance of 7.6Å which is well matched with the earlier report [17]. The XRD pattern of rGO decorated $CoSe_2$ nanocomposites well matches with the JCPDS CARD NO: **89-2003**. Compared with the pure $CoSe_2$, an additional peak observed at 2θ =23.40˚ indicates the presence of rGO [15]. The diffraction peaks are observed around 23.40˚, 29.59˚, 41.17˚, 43.55˚, 45.21˚, 51.55˚, 55.83˚, 61.40˚ and 65.05˚. From the X-ray diffraction analysis, it was observed that the nanocomposites belong to orthorhombic structure with lattice parameter a=4.840; b=5.720; c=3.600. The size of the crystallite (D) was estimated by applying Debye Scherrer's equation $D=0.9\lambda/\beta\cos\theta$. Here λ, β and θ are the wavelength of x-ray, full width at half maximum and peak position respectively. Employing this, the size of rGO decorated $CoSe_2$ nanocomposites was determined to be 18.63nm. Microstrain was calculated to be $5.56X10^{-3}$. Dislocation density was calculated to be $3.28X10^{-3}(nm)^{-2}$.

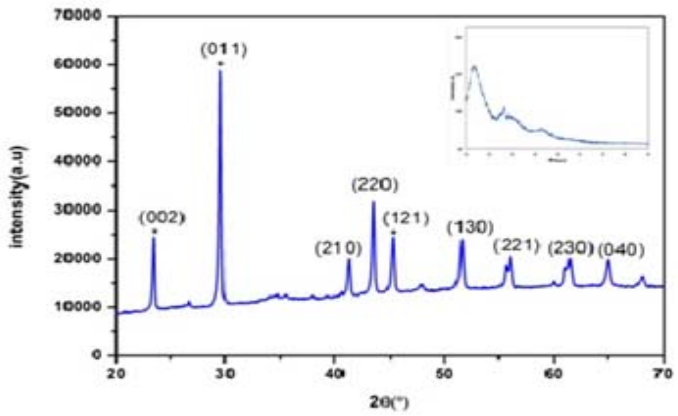

Fig.1. XRD pattern of GO and rGO decorated $CoSe_2$ nanocomposites

3.2. Morphology of rGO decorated $CoSe_2$ Nanocomposites

The surface morphology of the synthesized composites was examined by using SEM. Fig.2 shows the SEM images of the GO and rGO decorated $CoSe_2$ composites respectively. The morphology of GO shows flake -like structure. In rGO decorated $CoSe_2$ composites, it shows crumpled and folded rGO sheets can be seen clearly through the morphology of the composites. The $CoSe_2$ nanoparticles are tightly enfolded on the surface of the rGO sheets. During the growth of the rGO decorated $CoSe_2$ nanocomposites, the existence of the rGO sheets prevents $CoSe_2$ from agglomerating and empowers a good dispersion of these nanoparticles over the rGO sheets.

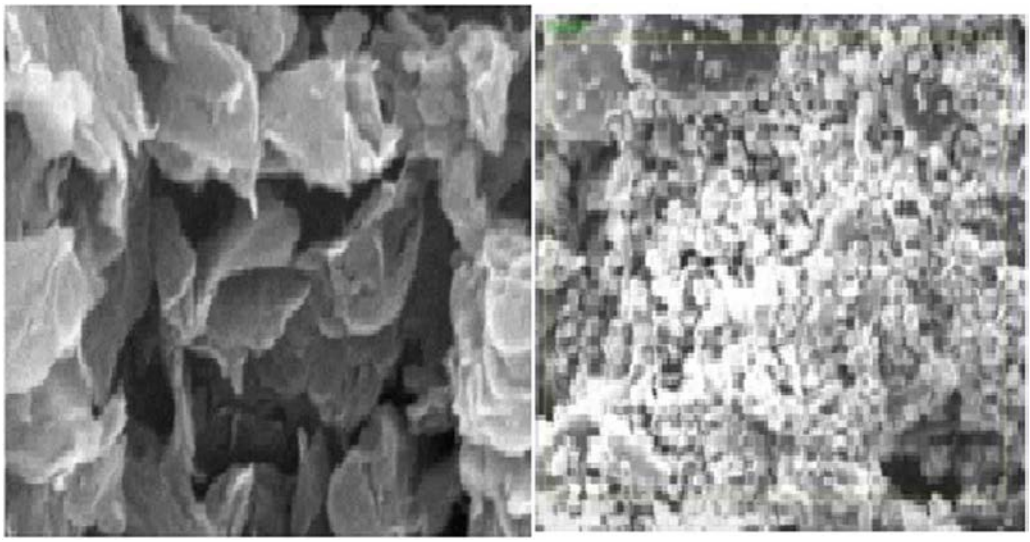

Fig. 2. SEM image of GO and rGO decorated $CoSe_2$ nanocomposites

3.3. EDAX analysis of rGO decorated $CoSe_2$ Nanocomposites

The EDAX spectrum of the rGO decorated $CoSe_2$ composites is shown in the fig.3. From the EDAX spectrum, it shows the C, O, Co and Se peaks at 0.3, 0.5, 0.8 and 1.4 keV respectively. The Carbon content of the reduced graphene oxide in the composites is 33.96%. The Oxygen content of the reduced graphene oxide in the composites is 16.25%. It was shown that some oxygen containing functional groups were still present in the composites. The Cobalt and Selenide present in the composites are 4.69 and 41.36% respectively. The composites were reduced by using reducing agent like hydrazine hydrate but there is no nitrogen content in the rGO decorated $CoSe_2$ composites. It shows that the composites have been obtained without any impurities. From this, EDAX spectrum confirms the presence of rGO decorated $CoSe_2$ composites.

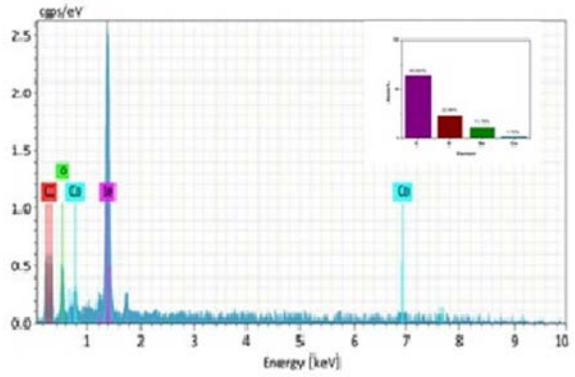

Fig. 3. EDAX spectrum of rGO decorated $CoSe_2$ nanocomposites

3.4. FTIR analysis of rGO decorated $CoSe_2$ Nanocomposites

The functional groups present in the nanocomposites were investigated by FTIR. The FTIR spectrum of the GO and rGO decorated cobalt selenide nanocomposites are shown in fig.4. The FTIR spectrum of GO shows multiple peaks because of extensive oxidation, the broad band at 3434cm^{-1} is due to the stretching vibrations of structural OH groups, the absorption bands corresponding to the C=O carbonyl stretching at 1728 cm^{-1} and the C=O stretching at 1226 and 1055 cm^{-1}. The band at 1406 cm^{-1} corresponds to the O-H deformation [18]. From the FTIR spectrum of the rGO decorated cobalt selenide nanocomposites, the band observed at 1980, 1551 and 1415cm^{-1} specifies the presence of C-O and C-C bond. The other peaks at 690 and 445 cm^{-1} corresponds to Co and Se. However, these peaks in the spectrum of rGO decorated cobalt selenide nanocomposites almost disappear, it suggests that all oxygen containing functional groups were removed during the reduction treatment. From the FTIR spectra it reveals that, the presence of rGO is clearly confirmed from the rGO peak around 1551 and 1415cm^{-1}. There is no corresponding OH peak in the composites which shows that the prepared nanocomposite is free from water molecules.

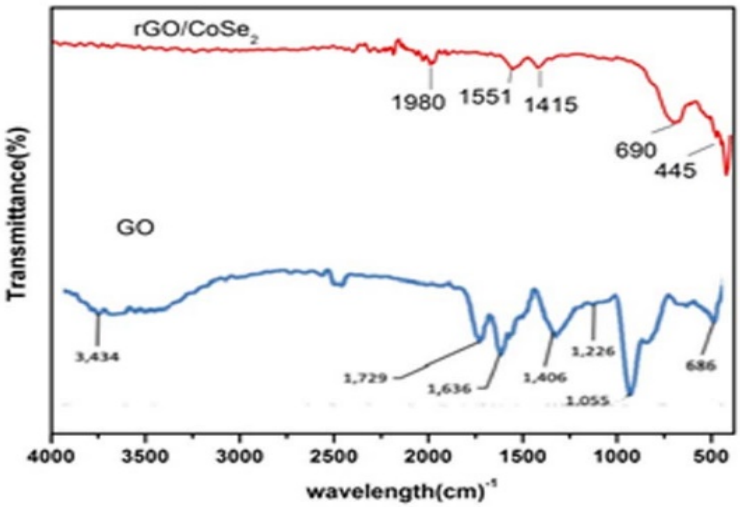

Fig. 4. FTIR spectra of GO and rGO decorated $CoSe_2$ nanocomposites

3.5 Optical analysis of rGO decorated $CoSe_2$ Nanocomposites

Optical measurement techniques such as spectrophotometer are powerful methods for the determination of the optical properties of nanocomposites. In most cases these methods are non-destructive and therefore very useful for calculation of optical parameters. The optical performance of the nanocomposites is significant to regulate its usage in optoelectronic devices. The optical properties of nanocomposites can be evolved mainly from its optical transparency, absorption coefficient, band gap, extinction coefficient and the refractive index. The optical properties of the nanocomposites are ruled by the interaction between the nanocomposites and the electric and magnetic fields of the electromagnetic wave. Optical constants of a material such as optical band gap and extinction coefficient is quite important to observe the material's potential optoelectronic applications. Further, the optical properties may also be closely associated to the material's atomic structure, electronic band structure and electrical properties [19].

3.5.1. Optical band gap

The optical transmittance spectrum of the prepared nanocomposites was shown in Fig. 5. From the fig.5, the lower cut-off wavelength of rGO decorated $CoSe_2$ nanocomposites was around 650 nm. The small peak appears at 213nm near UV region indicates the presence of rGO. The absorption coefficient (α) of nanocomposites was determined from optical transmittance measurement at room temperature. The value of α was estimated using the relation:

$$\alpha = (1/t) \ln (1/T) \quad (1)$$

where T is the transmittance and t are the thickness of the specimen. The relation connecting the absorption coefficient (α) and photon energy (hν) is

$$(\alpha h\nu)^n = A(h\nu - E_g) \quad (2)$$

where E_g is optical band gap of the nanocomposite and A is a constant [20]. Tau's plot is drawn using the above relation and optical band gap is found to be 1.4 eV.

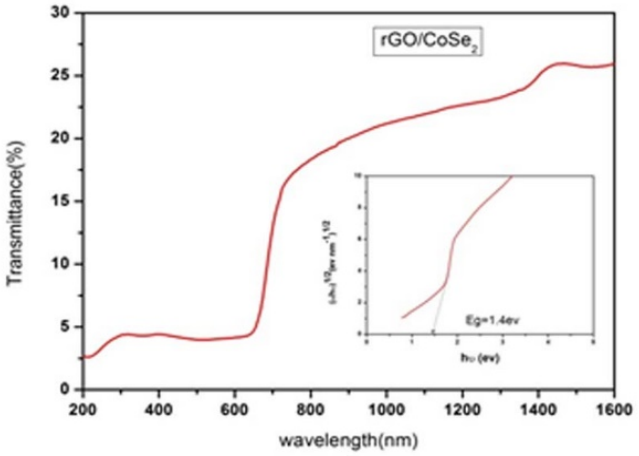

Fig. 5. Transmission spectrum and Tauc's plot of rGO decorated $CoSe_2$ nanocomposites

3.5.2. Absorbance and reflectance

Absorbance is a measure of the capacity of a substance or sample to absorb light of a specified wavelength and it is equal to the logarithm of the reciprocal of the transmittance. The absorbance can be calculated using the relation

$$A=\log(1/T) \quad (3)$$

where T is the transmittance [21].

Reflectance is a measure of the ability of a surface of the sample to reflect light. It is also known as reflectivity or reflectance coefficient [22]. The reflectance gives the ratio of the energy of reflected to incident light from prepared composites. Also, optical reflectance (R) is calculated from the relation

$$R = 1 - (A + T) \quad (4)$$

The absorbance and reflectance of rGO decorated $CoSe_2$ nanocomposites have been determined using the above equations in the wavelength range of 200–1600 nm. The variations of absorbance (%) and reflectance (%) with wavelength(nm) of the nanocomposites are shown in Fig.6. It is noticed from the results that the absorbance of the nanocomposites is low in the visible region up to the cut-off wavelength around 650 nm and this is the reciprocal of the transmittance. The reflectance is about 15% in the visible region up to the cut off wavelength. It is observed from the results that transmittance, reflectance and absorbance are equal to 100% at any wavelength.

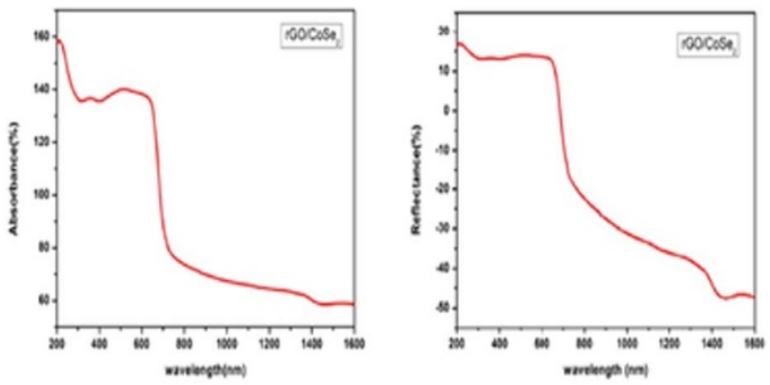

Fig. 6. Absorbance and reflectance spectrum of rGO decorated $CoSe_2$ nanocomposites

3.5.3. Extinction coefficient and refractive index

The extinction coefficient is the fraction of electromagnetic energy or light lost due to scattering and absorption per unit thickness or distance in a particular medium. In electromagnetic terms, the extinction coefficient can be described as the degeneration or restraining of the amplitude of the incident electric and magnetic fields. The extinction coefficient can be calculated from the following relation [23].

$$k=\lambda\alpha/4\pi \quad (5)$$

where λ is the wavelength of the incident radiation. The extinction coefficient as a function of wavelength and photon energy is presented in Fig.7 and 8. From the result, it is observed that the extinction coefficient (k) decreases with increase in wavelength near in the UV and visible region. The extinction coefficient decreases with the increase of photon energy. The low value of k is due to the weedy interaction between the photons and electrons in the composites.

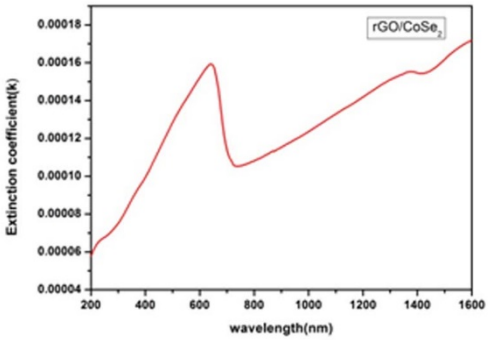

Fig. 7. Variation of the extinction coefficient versus the wavelength for rGO decorated $CoSe_2$ nanocomposites,

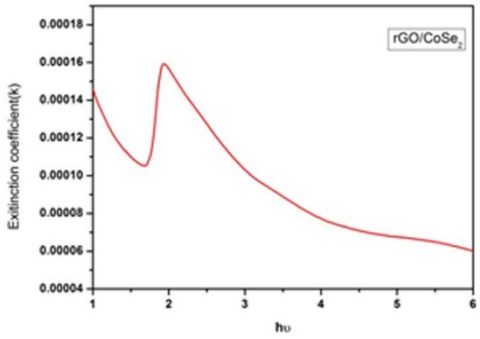

Fig. 8. Variation of the extinction coefficient versus photon energy for rGO decorated $CoSe_2$ nanocomposites

3.5.4. Refractive index

The refractive index is a measure of the speed of light in the substance. It is expressed as a ratio of the speed of light in vacuum to that medium. The refractive index can be calculated by the following relation:

$$n = 1 + \sqrt{R} / 1 - \sqrt{R} \quad (6)$$

From the fig.9 and 10, it is detected that the refractive index decreases with increasing wavelength and increases with increasing photon energy. The change in refractive index with variation of wavelength of the incident light beam is due to the interaction between the photons and electrons. By modifying the photon energy, one can accomplish a desired material for the device fabrication such as electro optic and optoelectronic devices [24].

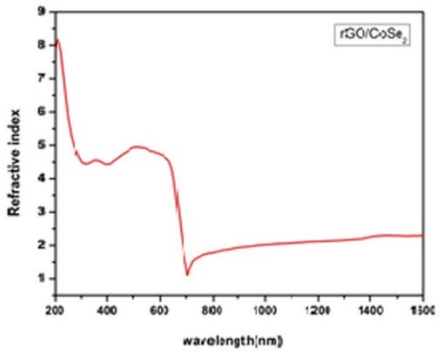

Fig. 9. Plot of the refractive index as a function of wavelength for rGO decorated $CoSe_2$ nanocomposites

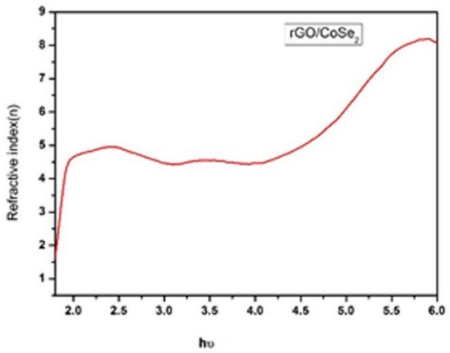

Fig. 10. Plot of the refractive index as a function of photon energy for rGO decorated $CoSe_2$ nanocomposites

3.5.5. Optical conductivity

Optical conductivity (σ_{op}) is one of the parameters for learning the electronic states. If a sample is subjected to an external electric field then redistribution of charges occurs and current present in it is induced. For small fields, the induced polarization and current are proportional to the inducing field. The optical conductivity of the nanocomposites was calculated using the following relation [25].

$$(\sigma_{op})=\alpha nc/4\pi \quad (7)$$

where c is the velocity of light. α is the absorption coefficient and n is the refractive index.

Fig.11 and 12 shows the variation of the optical conductivity as a function of wavelength and photon energy for the nanocomposites. From the figure, optical conductivity increases with increase in photon energy for nanocomposites under investigation. Nanocomposites shows high magnitude of optical conductivity and this confirms the presence of high photon response of the composites and this possessions makes the composites more prominent for device applications in information processing and computing. For larger energy values, an exponential rise was observed in the optical conductivity of the nanocomposites. This can be explained in terms of transfer of charge carriers from the valence to conduction band in the nanocomposites. Thus, a rapid increase in optical conductivity is detected at 1.4 eV provides the accuracy of energy band gap calculations.

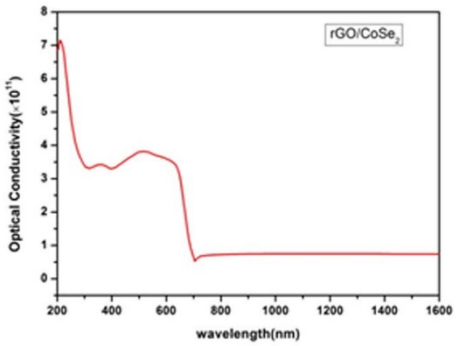

Fig. 11. Plot of optical conductivity as a function of wavelength for rGO decorated $CoSe_2$ nanocomposites

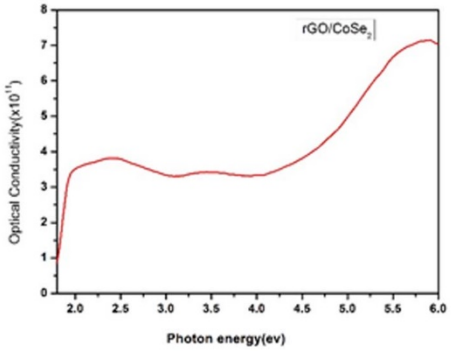

Fig. 12. Plot of optical Conductivity as a function of photon energy for rGO decorated $CoSe_2$ nanocomposites

3.5.6. Dielectric constant

The dielectric constant is proportional to polarizability of the nanocomposites. It expresses the electrical equivalent of relative magnetic permeability when subjected to the electric flux. Dielectric constant is treated as a complex function of the frequency of the applied field and the complex dielectric constant (ε_c) symbolizes the optical properties of the nanocomposites and is calculated using the expression as given below

$$\varepsilon_c = \varepsilon_r + i\varepsilon_i = (n + ik)^2 \quad (8)$$

where ε_r and ε_i are the real and imaginary part of the dielectric constant respectively. The real and imaginary parts of dielectric constant are related to the refractive index and extinction coefficient as given below,

$$\varepsilon_r = n^2 - k^2 \quad (9)$$

The variations of these two parameters (ε_r and ε_i) with photon energy are shown in fig.13. The values of real part increase with photon energy but the imaginary part of the dielectric constant decreases with photon energy and then increases. The prepared nanocomposite is associated with low value of imaginary part of dielectric constant which inhibits the propagation

electromagnetic (EM) energy which has aided conductivity. The low dielectric constant of the nanocomposites fulfill the essential requirement of the optoelectronic applications.

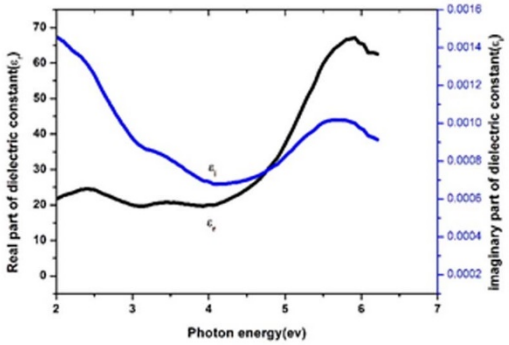

Fig. 13. Plot of dielectric constant as a function of photon energy for rGO decorated $CoSe_2$ nanocomposites

4. Conclusions

Reduced Graphene oxide decorated Cobalt Selenide (rGO/$CoSe_2$) was synthesized via a facile hydrothermal method. The lattice dimensions were determined from the XRD technique and found that the nanocomposites belong to the orthorhombic structure with lattice parameter a=4.840; b=5.720; c=3.600. The Grain size, Microstrain and Dislocation density of the composites were calculated. The FTIR spectrum confirms the oxygen removal in the nanocomposites. From UV transmittance study, the band gap was found to be 1.4ev. The optical constants of the prepared composites such as extinction coefficient, refractive index and optical conductivity was calculated and confirms its suitability for optical device fabrication. The real and imaginary part of the dielectric constant were evaluated. Addition of rGO to the cobalt selenide, decreases the particle size that it is expected to further increase the specific capacitance.

Acknowledgements

The authors acknowledge Department of Physics, St.Xavier's College for constant encouragement in carrying out the present investigation.

Reference

[1] Raluca Tarcan (2020). Reduced graphene oxide today. Journal of Materials Chemistry C, (4), 1198-1224. doi:10.1039/C9TC04916A.
[2] Wallace, P. R. (1947). The Band Theory of Graphite. Physical Review, 71(9), 622-634. doi:10.1103/physrev.71.622
[3] Geim, A. K. (2009). Graphene: Status and Prospects. Science, 324(5934), 1530-1534. doi:10.1126/science.1158877

[4] Thangamuthu, M., Hsieh, K. Y., Kumar, P. V., & Chen, G. (2019). Graphene- and Graphene Oxide-Based Nanocomposite Platforms for Electrochemical Biosensing Applications. International Journal of Molecular Sciences, 20(12), 2975. doi:10.3390/ijms20122975

[5] P. Suvarnaphaet and S. Pechprasarn , Graphene-Based Materials for Biosensors: A Review. (2017). Sensors, 17(10), 2161. doi:10.3390/s17102161

[6] Nikam, A. N., More, M. P., Pandey, A. P., Patil, P. O., Patil, A. G., & Deshmukh, P. K. (2019). Design and development of thiolated graphene oxide nanosheets for brain tumor targeting. International Journal of Polymeric Materials and Polymeric Biomaterials, 69(10), 611-621. doi:10.1080/00914037.2019.1596911

[7] Shi S, Yang K, Hong H, Chen F, Valdovinos HF, Goel S, Barnhart TE, Liu Z, Cai W. VEGFR targeting leads to significantly enhanced tumor uptake of nanographene oxide in vivo. Biomaterials. 2015 Jan;39:39-46. doi: 10.1016/j.biomaterials.2014.10.061. Epub 2014 Nov 15. PMID: 25477170; PMCID: PMC4258896.

[8] Raluca Tarcan (2020). Reduced graphene oxide today. Journal of Materials Chemistry C, (4), 1198-1224. doi:10.1039/C9TC04916A.

[9] Rabchinskii, M.K., Dideikin, A.T., Kirilenko, D.A. et al. Facile reduction of graphene oxide suspensions and films using glass wafers. Sci Rep 8, 14154 (2018). https://doi.org/10.1038/s41598-018-32488-x

[10] Jiang, K., Liu, B., Luo, M. et al. Single platinum atoms embedded in nanoporous cobalt selenide as electrocatalyst for accelerating hydrogen evolution reaction. Nat Commun 10, 1743 (2019). https://doi.org/10.1038/s41467-019-09765-y

[11] Liao, M., Zeng, G., Luo, T., Jin, Z., Wang, Y., Kou, X., & Xiao, D. (2016). Three-dimensional coral-like cobalt selenide as an advanced electrocatalyst for highly efficient oxygen evolution reaction. Electrochimica Acta, 194, 59-66. doi: 10.1016/j.electacta.2016.02.046

[12] Liao, M., Zeng, G., Luo, T., Jin, Z., Wang, Y., Kou, X., & Xiao, D. (2016). Three-dimensional coral-like cobalt selenide as an advanced electrocatalyst for highly efficient oxygen evolution reaction. Electrochimica Acta, 194, 59-66. doi: 10.1016/j.electacta.2016.02.046

[13] Gaur, M. L., Hankare, P. P., Garadkar, K. M., Mulla, I. S., & Bhuse, V. M. (2014). Morphological and optoelectronic studies on poly-crystalline leaf-like cobalt selenide thin film synthesized using a chemical bath deposition technique. New J. Chem., 38(1), 255-259. doi:10.1039/c3nj00924f

[14] Jahangir Masud, Abdurazag T. Swesi, Wipula P. R. Liyanage, and Manashi Nath. (2016) Cobalt Selenide Nanostructures: An Efficient Bifunctional Catalyst with High Current Density at Low Coverage. ACS.Appl. Mater.Interfaces,8, 17292-17302.doi:10.1021/acsami.6b04862

[15] Zhangpeng Li, Hongtao Xue, Reduced Graphene Oxide/Marcasite type cobalt selenide nanocrystals for lithium ion batteries with excellent cyclic performance.ChemElectroChem. doi:10.1002/celc.201500179

[16] Firdaus,F., Noor -e-Iram, Khan, M.S.et al. Facile synthesis, Characterization and Photocatalytic Activity of Band Gap Engineered Cobalt Selenide Nanoparticles. Arab J Sci Eng 41, 2377-2384 (2016). doi:101007//s13369-016-2100-z

[17] Gurunathan, S., Han, J. W., Daye, A. A., Eppakayala, V., & Kim, J. (2012). Oxidative stress-mediated antibacterial activity of graphene oxide and reduced graphene oxide in Pseudomonas aeruginosa. International Journal of Nanomedicine, 5901. doi:10.2147/ijn.s37397

[18] Hanifah, M. F., Jaafar, J., Aziz, M., Ismail, A. F., Rahman, M. A., & Othman, M. H. (2015). Synthesis of Graphene Oxide Nanosheets via Modified Hummers' Method and Its Physicochemical Properties. Journal Teknologi, 74(1). doi:10.11113/jt.v74.3555

[19] Shanthi, D., Selvarajan, P., & Perumal, S. (2016). Growth, linear optical constants and photoluminescence characteristics of beta-alaninium picrate (BAP) crystals. Optik, 127(6), 3192-3199. doi:10.1016/j.ijleo.2015.11.189

[20] Tauc, J. (1974). Optical Properties of Amorphous Semiconductors. Amorphous and Liquid Semiconductors, 159-220. doi:10.1007/978-1-4615-8705-7_4

[21] M. Mazhdi, J. Saydi, M. Karimi, J. Seidi, F. Mazhdi, A study on optical, photoluminescence and thermoluminescence properties of ZnO and Mn doped-ZnO nanocrystalline particles, Optik 124 (20) (2013) 4128–4133

[22] M. Srivastava, A.K. Ojha, S. Chaubey, A. Materny, Synthesis and optical characterization of nanocrystalline NiFe2O4 structures, J. Alloys Compd. 481 (1–2) (2009) 515–519.

[23] B.K. Periyasamy, R.S. Jebas, N. Gobalakrishnan, T. Balasubramanian, Development of NLO tunable band gap organic devices for optoelectronic applications,Mater. Lett. 61 (21) (2007) 4246–4249

[24] John Jain, P. Christuraj, K. Anitha, T. Balasubramanian, Band gap enhancement on metal chelation: growth and characterization of cobalt chelated glycine single crystals for optoelectronic applications, Mater. Chem. Phys. 118 (2–3) (2009) 284–287.

[25] Tanusri Pal, Tanusree Kar, Studies of microhardness anisotropy and Young's modulus of nonlinear optical crystal l-arginine hydrochlorobromo monohydrate, Mater. Lett. 59 (11) (2005) 1400–1404